

Numerical Simulations of Oscillation Modes of the Solar Convection Zone

D. Georgobiani¹, A.G. Kosovichev², R. Nigam^{2,3}, A. Nordlund⁴, R.F. Stein¹

ABSTRACT

We use the three-dimensional hydrodynamic code of Stein and Nordlund to realistically simulate the upper layers of the solar convection zone in order to study physical characteristics of solar oscillations. Our first result is that the properties of oscillation modes in the simulation closely match the observed properties. Recent observations from SOHO/MDI and GONG have confirmed the asymmetry of solar oscillation line profiles, initially discovered by Duvall et al. In this paper we compare the line profiles in the power spectra of the Doppler velocity and continuum intensity oscillations from the SOHO/MDI observations with the simulation. We also compare the phase differences between the velocity and intensity data. We have found that the simulated line profiles are asymmetric and have the same asymmetry reversal between velocity and intensity as observed. The phase difference between the velocity and intensity signals is negative at low frequencies and jumps in the vicinity of modes as is also observed. Thus, our numerical model reproduces the basic observed properties of solar oscillations, and allows us to study the physical properties which are not observed.

Subject headings: Sun: interior — Sun: oscillations — convection — methods: numerical

¹Physics and Astronomy Department, Michigan State University, East Lansing, MI 48824-1116

²W.W.Hansen Experimental Physics Laboratory, Stanford University, Stanford, CA 94305-4085

³Department of Mathematics, Stanford University, Stanford, CA 94305-2125

⁴Teoretisk Astrofysik Center, Danmarks Grundforskningsfond, Juliane Maries Vej 30, DK-2100 København Ø, Denmark

1. Introduction

The peaks of solar oscillation modes observed in velocity and intensity power spectra are asymmetric (Duvall et al. 1993). Moreover, the asymmetry between the velocity and intensity line profiles is reversed. This latter was a puzzling result, and it was initially thought to be an error in the observations (Abrams & Kumar 1996). However, recently it was confirmed by SOHO/MDI observations (Nigam et al, 1998). The velocity power spectrum has negative asymmetry (more power on the low frequency side of the peak), while the intensity power spectrum has positive asymmetry (more power on the high frequency side of the peak). In general, the asymmetry is a result of excitation of solar oscillations by a localized source. It originates from the interference of direct waves from the source with waves that start inward and are refracted back out. The asymmetry is a strong function of frequency, and varies weakly with angular degree ℓ . The reversal of asymmetry between velocity and intensity is due to the presence of correlated background noise, whose level depends on characteristics of granulation (Nigam et al, 1998). Since the model of Nigam et al (1998) is a phenomenological one, the physics of the correlated noise is not yet fully understood. Roxburgh & Vorontsov (1997) proposed that the reversal in asymmetry occurs in velocity. Observations suggest that the reversal occurs in intensity as proposed by Nigam et al (1998). It is therefore desirable to test these ideas. Realistic 3D hydrodynamic simulations of upper layers of the solar convection zone (e.g., Stein & Nordlund, 1989; Stein & Nordlund, 1998) have p and f modes with similar asymmetries and asymmetry reversals as the observed modes. These simulations can therefore be used to study the characteristics of the correlated noise.

Another interesting property of solar oscillation modes is the phase difference between velocity and intensity, which was first observed by Deubner & Fleck (1989) and studied theoretically by Marmolino & Severino (1991). It may provide an useful diagnostic of the excitation mechanism of the oscillations. Severino et al. (1998), Straus et al. (1998), Oliviero et al. (1999) and Nigam & Kosovichev (1999) attribute the phase behavior to the interaction of the correlated background with the oscillations. These phase relations can also be studied using the realistic hydrodynamic simulations of the near surface layers of the Sun.

2. Numerical Model of Convection

We use the numerical code of Stein and Nordlund (1998) to make a physically realistic three-dimensional simulation of the shallow upper layers of the solar convective zone. The code solves the compressible hydrodynamic equations and includes ionization in the equation of state and LTE radiative transfer in the energy balance. The horizontal boundary conditions are periodic, while the top and bottom boundaries of the computational domain are transmitting. The horizontal size of the domain is 6 by 6 Mm. It ranges in depth from 2.5 Mm below the $\tau = 1$ surface to 0.5 Mm above it, reaching the height of the temperature minimum of the solar atmosphere. The computational grid of $63 \times 63 \times 63$ mesh points gives a spatial resolution of $100 \text{ km} \times 100 \text{ km}$ horizontally and $35 - 90 \text{ km}$ vertically. The system becomes thermally relaxed after several turnover times (a turnover time is approximately 1 hour). We have generated data for 43 hours of solar time, which provide $6.4 \mu\text{Hz}$ frequency resolution. We calculate power spectra of the velocity and intensity and their phase differences to study properties of the oscillations generated in this simulation box. In the simulation, the first set of nonradial modes corresponds to a harmonic degree $\ell = 740$ (or $k_h = 1 \text{ Mm}^{-1}$), the second set corresponds to $\ell = 1480$ ($k_h = 2 \text{ Mm}^{-1}$) etc.

3. Calculation of the Power Spectra

Solar oscillations in velocity and intensity are measured from the Ni I 6768Å absorption line which is formed about 200–300 km above the photosphere. The MDI instrument on SOHO spacecraft records filtergrams (intensity images at five wavelengths) which span the absorption line. The velocity signal is obtained by differencing the filtergrams on opposite sides of the line which is sensitive to Doppler shift and minimizes the effect of intensity fluctuations. The intensity signal is obtained by summing the filtergrams in a way to approximate the continuum intensity in the vicinity of the spectral line and minimize the effects of Doppler shifts (Scherrer et al. 1995). For the comparison with the numerical simulations, we use a time series of the spherical harmonic transform of the full-disk data for $\ell = 740$. The effect of solar differential rotation is removed; and the oscillation power spectra are summed over all $2\ell + 1$ m values. We note that MDI measures the continuum intensity in the vicinity of the Ni I 6768Å line, which is different

from the broad-band continuum data obtained from the simulations. This might be a source of some of the divergences between the model and the observations.

In the numerical model, the vertical component of velocity, $V(x, y, t)$, is calculated at a height of 200 km above the $\tau = 1$ surface, close to the formation height of the observed MDI Doppler velocities. The simulated continuum intensity (the emergent continuum specific intensity), $I(x, y, t)$, is calculated by solving the Feautrier equation along a vertical ray, in LTE, using an opacity distribution function. To extract the nonradial modes we multiply $V(x, y, t)$ and $I(x, y, t)$ by $\sin(k_x x)$, $\sin(k_y y)$, $\cos(k_x x)$ and $\cos(k_y y)$, where k_x or k_y are horizontal wave numbers equal to $2\pi n/L$, where $L = 6$ Mm is the horizontal dimension of the simulation box (the same for both x and y directions), and $n = 1, 2, 3, \dots$ is the number of nodes in horizontal direction. Then we average the products of V and I with these sines and cosines over the horizontal planes. This corresponds to the 2-dimensional Fourier transform of the data with specific horizontal wave numbers. We then take Fourier transforms in time to obtain the power spectra, $\tilde{V}(k_x, k_y, \omega)$ and $\tilde{I}(k_x, k_y, \omega)$, and sum these four different spectra to obtain a power spectrum for a particular horizontal wave number $k_h^2 = k_x^2 + k_y^2$. This corresponds to summing the observational power spectra over azimuthal degree m . Since the line profiles for $k_h = 2 \text{ Mm}^{-1}$ ($\ell = 1480$) and higher are rather noisy, we present the results for $k_h = 1 \text{ Mm}^{-1}$ ($\ell = 740$) only. The $k_h = 1 \text{ Mm}^{-1}$ spectra are obtained either for $n_x = 1$ and $n_y = 0$ or $n_x = 0$ and $n_y = 1$. The modulus and phase of the cross spectra $\tilde{I}\tilde{V}^*$ give the coherence and phase difference between intensity and velocity.

4. Comparison between the Observed and Simulated Power Spectra

In Figures 1 and 2 we compare the observed and simulated mode power spectral densities in velocity and intensity for $\ell = 740$. The observational data represent 5 days of the observations of a quiet-sun region with a spatial resolution of 2 arcsec/pixel ($\sim 1,500$ km) and temporal resolution 1 min. The simulation data are for the lowest non-radial mode of the same angular degree, $\ell = 740$ ($k_h = 1 \text{ Mm}^{-1}$) calculated from a 43 hour run with a horizontal grid spacing of 100 km and time spacing of 0.5 min. In order to make our comparison more appropriate, we took only 43 hours of the observational data and every other

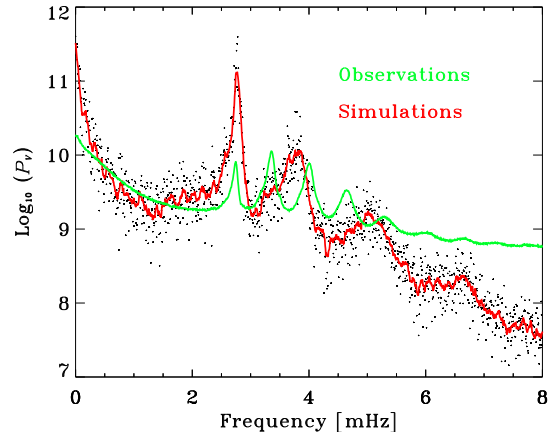


Fig. 1.— Observed and simulated velocity power spectral density for $\ell = 740$ from the SOHO/MDI (green curve) and for the first non-radial mode of a simulation of solar surface convection (dots and red curve). Units are $(\text{cm/s})^2/\text{Hz}$. Observed velocities are from the Doppler shifts of the NiII 6768 Å line summed over all $2\ell + 1$ m modes. Simulated velocities are from a calculation on a domain 6×6 Mm horizontally \times 2.5 Mm deep, spanning 43 hours of solar time, summed over the 4 modes with 6 Mm horizontal wavelength. The simulated modes are sparser and broader than the observed modes because the simulated domain is shallower than the turning points of the observed modes, resulting in a smaller mass and larger amplitude for the simulated modes.

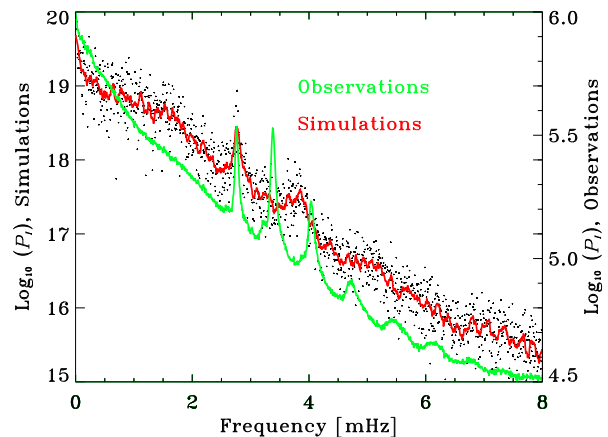


Fig. 2.— Observed and simulated intensity power spectral density for the same case as the velocity in Figure 1. Observed intensity power spectral density is in units of $(\text{CCD counts per sec})^2/\text{Hz}$. Simulated intensity power spectral density is in units of $(\text{erg/cm}^2/\text{s/ster})^2/\text{Hz}$.

snapshot in the simulated data to have the same 1 min time step as in observations. The simulated and

observed velocity power are similar between the peaks at low frequency, but the peak power is larger in the simulation than the observations because the same excitation and damping processes are supplying energy to fewer modes with smaller mode mass. The simulation power also falls off much more rapidly at high frequencies, probably due to the low resolution of the simulation. The frequency separation between the simulated modes is larger than the separation between the observed modes because of the shallow computational domain. It is only 2.5 Mm deep, whereas $\ell = 740$ modes in the Sun have the turning points below ~ 4 Mm. As a result, the resonant frequencies in the simulation are different from the frequencies of solar modes. Also, the simulated modes have less inertia and larger amplitudes than the solar modes. Because of the smaller inertia (mode mass) the damping rate is much larger in the simulation than the Sun, so the simulated line profiles are broader than the observed ones. However, these differences do not prevent us from studying the mode physics with the numerical simulations.

The lowest frequency mode in the power spectra is the f mode, which is essentially a surface gravity mode. It does not exist in radial oscillations, but in the nonradial data, it is very strong and shows the same asymmetry behavior as do p modes. Interestingly enough, in the simulations the amplitude of the f mode is greater than the amplitudes of the p modes, whereas in the observational data the f-mode amplitude is smaller than the amplitude of the p_1 mode.

For both the simulations and the observations the velocity and intensity line profiles are clearly asymmetric, with opposite asymmetries in velocity and intensity (Figures 1 and 2). Also, the slopes of the power spectra in velocity and intensity have a power law behavior in both the simulation and observations.

5. Comparison between the Observed and Simulated Intensity - Velocity Phase Difference.

Figure 3 compares the observed and simulated phase differences between the intensity and velocity signals, $I - V$, as a function of frequency. Both the observations and simulations have negative phase difference $I - V$ at low frequency. In both cases, the phase difference departs from the 90° phase difference predicted by the adiabatic theory of trapped standing waves. In both cases, there are jumps in phase of

$\sim 90^\circ$ at the mode frequencies. The phase differences approach zero for high frequency propagating waves as expected for adiabatic acoustic waves.

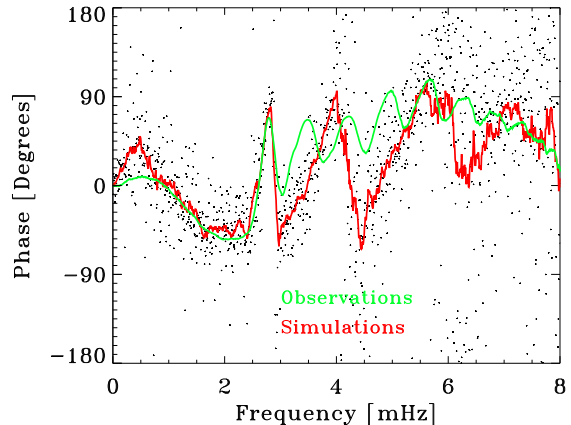


Fig. 3.— Observed and simulated intensity - velocity phase difference. The observed data are from SOHO/MDI with $\ell = 740$ summed over all $2\ell+1$ m values. The simulated data are for the first non-radial mode (with horizontal wavelength 6 Mm). The phase jumps $\sim 90^\circ$ at the mode resonant frequencies where the oscillation amplitude is large.

6. Discussion

Mode asymmetry in the spectral domain is a result of the interference pattern of waves from a localized source not being symmetrical relative to the mode resonant frequencies. Constructive and destructive interference occurs between waves from the source that propagate outward with those that propagate inward and are refracted outward. Destructive interference causes characteristic “troughs” on one side of the modal lines, where the amplitude is minimal. The frequencies of the “troughs” depend on the source location and type (Duvall et al. 1993, Vorontsov et al. 1998, Nigam and Kosovichev, 1999). In the solar case, the destructive interference occurs at frequencies slightly higher than the resonant frequencies. This corresponds to the negative line asymmetry. The interference pattern may be also affected by the presence of an additional signal correlated with the source. Variations of the continuum intensity in the convective granules, which are associated with the process of excitation of solar oscillations, are such a signal (Nigam et al., 1998). This correlated signal shifts the frequencies of the “troughs”. If the correlated signal is sufficiently strong the “troughs” may be shifted

to the other side of the mode resonant frequencies, and thus reverse the asymmetry of the modal lines. This reversal of the asymmetry is observed in both the MDI intensity data and the intensity spectra obtained in the numerical simulations. The numerical results allow us to verify that variations in the background intensity in the granules are indeed correlated with the oscillations (Nordlund and Stein 1998). In the MDI Doppler velocity measurements this correlated variation is essentially cancelled by taking differences of values on opposite sides of the line. In the intensity measurement it is enhanced by summing contributions from opposite sides of the line. The correlated component of the noise must be large enough to reverse the asymmetry in the intensity power spectrum, but not sufficiently large to reverse the asymmetry in the velocity power spectrum (Nigam et al. 1998).

These results are consistent with the observations of Goode et al. (1998), where it appears that the acoustic events occur in cool and narrow intergranular dark lanes. Prior to an acoustic event there is darkening in the intensity. This darkening is also correlated to the strength of the event. Strong events are preceded by longer darkening. The reversal of asymmetry in intensity due to a correlated background has been confirmed by Kumar & Basu (1999) and Rast (1999). However, there is, as yet, no complete theory of the influence of the background variations on the observed properties of solar oscillations.

The variations of the phase difference between the intensity and velocity signals with frequency can also be explained by the presence of the correlated noise (Nigam & Kosovichev 1999). The intensity - velocity cross spectrum is the product

$$C_{I-V} = (\delta I + N_I)(\delta V + N_V)^* + N_{I\text{uncorr}}N_{V\text{uncorr}} ,$$

and the intensity - velocity phase difference is

$$\tan \Theta_{I-V} = \Im C_{I-V} / \Re C_{I-V} .$$

Away from a mode the noise contribution dominates, while at an eigenfrequency the mode amplitude is large and dominates. If the intensity and velocity are nearly 90° out of phase, as they are expected to be for adiabatic waves, then they will contribute primarily to the imaginary part in the numerator, but have little effect on the denominator. At the mode eigenfrequency there will be a large jump in mode amplitude, producing a large jump in the ratio $\tan \Theta_{V-I}$, and hence a change in Θ of order $\sim 90^\circ$.

The phase and asymmetry behavior of the modes constrains the nature of the excitation mechanism of solar oscillations.

7. Conclusions

In this Letter, we have compared observed asymmetries of the oscillation line profiles in the velocity and intensity power spectra with those obtained in 3D hydrodynamic simulations of solar convection. The basic characteristics of the observed mode peak asymmetries are reproduced in the simulations: the modes are asymmetric, with the velocity and intensity having opposite asymmetries. The reversal in asymmetry occurs in the intensity signal (possibly due to the process of radiative transfer, which causes additional signal in the intensity fluctuations correlated with the oscillation). This is consistent with the result of Nigam et al (1998). This is an important step in studying the physical properties of solar oscillations and their interaction with turbulence. The basic characteristics of the observed intensity - velocity phase difference are also reproduced in the simulations. The similarity of the oscillation mode properties in the simulation and observations means that the simulations can be used to investigate the origin of mode behavior.

This work was supported by the SOI-MDI NASA contract NAG5-3077 at Stanford University and by NASA grant NAG 5-4031 and NSF grant AST 9521785 to MSU. D.G. expresses her gratitude to Sasha Kosovichev for the possibility of performing a part of this work at Stanford, and to Maurizio Oliviero for useful discussions on phase differences. The calculations were performed at Michigan State University and the National Center for Supercomputing Applications. SOHO is a project of international cooperation between ESA and NASA.

REFERENCES

- Abrams, D., & Kumar, P. 1996, ApJ, 472,882
- Deubner, F.-L., & Fleck, B. 1989, Astronomy and Astrophysics, 213, 423
- Duvall, T.L., Jr., Jefferies, S.M., Harvey, J.W., Osaki, Y., & Pomerantz, M.A. 1993, ApJ, 410, 829
- Goode, P.R., Strous, L.H., Rimmele, T.R., & Stebbins, R.T. 1998, ApJ, 495, L27
- Kumar, P., & Basu, S. 1999, ApJ, 519, 389

- Marmolino, C., & Severino, G. 1991, *Astronomy and Astrophysics*, 242, 271
- Nigam, R., & Kosovichev, A.G. 1998, *ApJ*, 505, L51
- Nigam, R., & Kosovichev, A.G. 1999, *ApJ*, 510, L149
- Nigam, R., Kosovichev, A.G., Scherrer, P.H., & Schou, J. 1998, *ApJ*, 495, L115
- Nordlund, Å. & Stein, R.F. 1998, in F. L. Deubner, J. Christensen-Dalsgaard, & D. Kurtz, (eds.) *New eyes to see inside the sun and stars : pushing the limits of helio- and asteroseismology with new observations from the ground and from space*, IAU Symp 185, (Kluwer:Dordrecht) 199
- Oliviero, M., Severino, G., Straus, T., Jefferies, S.M., & Appourchaux, T. 1999, *ApJ*, 516, L45
- Rast, M.P. 1999, *ApJ*, in press
- Roxburgh, I.W., & Vorontsov, S.V. 1997, *MNRAS*, 292, L33
- Scherrer, P.H., Bogart, R.S., Bush, R.I., Hoeksema, J.T., Kosovichev, A.G., Schou, J., et al. 1995, *Solar Physics*, 162, 129
- Severino, G., Straus, Th., & Jefferies, S. M. 1998, in *SOHO 6/GONG 98 Workshop, Structure and Dynamics of the Interior of the Sun and Sun-like Stars*, Vol. 1, ed. S. Korzennik & A. Wilson (ESA SP-418; Noordwijk: ESA), 53
- Stein, R. F., & Nordlund, A. 1989, *ApJ*, 342, L95
- Stein, R. F., & Nordlund, A. 1998, *ApJ*, 499, 914
- Straus, T., Fleck, B., Severino, G., Deubner, F.-L., Marmolino, C., & Tarbell, T. 1998, in E.R.Priest (ed.), *A Crossroads for European Solar and Heliospheric Physics: Recent Achievements and Future Mission Possibilities*, Tenerife, ESA SP-417, 293
- Vorontsov, S. V., Jefferies, S. M., Duvall, T. L., & Harvey, J. W., 1998, *MNRAS*, 298, 464